Evaluation of Electron Donor Materials for Solution-Processed Organic Solar Cells via a Novel Figure of Merit

Jie Min, Yuriy N. Luponosov, Chaohua Cui, Bin Kan, Haiwei Chen, Xiangjian Wan, Yongsheng Chen, Sergei A. Ponomarenko, Yongfang Li, and Christoph J. Brabec*

Organic photovoltaic (OPV) technology offers many advantages, although no commercial applications have been achieved after more than a decade of intensive research and development. Several challenges have yet to be overcome including high power conversion efficiency (PCE), good processability, low cost, and excellent long-term stability, and so on. In this article, these fundamental challenges are significantly addressed by surveying and analyzing a new merit factor for material applied accessibility containing three parameters: synthetic complexity, device efficiency, and photostability. Thirty-five donor small molecules are introduced to assess their synthetic accessibility. Furthermore, the PCEs and device photostability of these molecules are carried out, and further measured under one sun illumination within 200 h, respectively. Combining with the characteristics of these three factors, investigated molecules are ranked according to an industrial figure of merit (i-FOM), while some guidelines for the material design and synthesis are given. It is suggested that a PCE of >14% and an i-FOM of >20% via active material engineering are realistic for possible industry future of OPV. Along with the systematic study, it is believed that this i-FOM can be taken into consideration at an early stage of molecular design and provides valuable insight for efficient evaluation of photovoltaic materials for possible commercial applications.

1. Introduction

As an important source of renewable energy for a sustainable future, thin-film solution-processed organic photovoltaics (OPVs) have received significant attention due to the advantages of lightweight, mechanical flexibility, low cost, and facile fabrication of roll-to-roll processing as well as substrate and shape freedom.[1–4] During the last two decades, photovoltaic materials are rapidly showing improvements in power conversion efficiencies (PCEs) of over 11% in the OPVs for small area devices (mm^2 scale) with the most promising bulk heterojunction (BHJ) configuration.[5–9] Despite this progress, the widespread commercial application of OPVs has yet to become a reality, and until now only prototypes and demo products with low PCEs of ≈2%–4% have been reported.[10–12] Several fundamental challenges with respect to the product cost, photovoltaic performance, long-term stability, etc., still hamper the up-scale

Prof. J. Min
The Institute for Advanced Studies
Wuhan University
Wuhan 430072, China
E-mail: Min.Jie@whu.edu.cn

Prof. J. Min, H. Chen, Prof. C. J. Brabec
Institute of Materials for Electronics and Energy Technology (I-MEET)
Friedrich-Alexander University Erlangen-Nuremberg
Martensstraße 7, 91058 Erlangen, Germany

Dr. Y. N. Luponosov, Porf. S. A. Ponomarenko
Enikolopov Institute of Synthetic Polymeric Materials
of the Russian Academy of Sciences
Profsoyuznaya st. 70, Moscow 117393, Russia

Dr. C. Cui, Prof. Y. Li
Laboratory of Advanced Optoelectronic Materials
College of Chemistry
Chemical Engineering and Materials Science
Soochow University
Suzhou 215123, China

DOI: 10.1002/aenm.201700465

B. Kan, Prof. X. Wan, Prof. Y. Chen
State Key Laboratory and Institute of Elemento-Organic Chemistry
Collaborative Innovation Center of Chemical Science
and Engineering (Tianjin)
Nankai University
Tianjin 300071, China

B. Kan, Prof. X. Wan, Prof. Y. Chen
Key Laboratory of Functional Polymer Materials and the Centre
of Nanoscale Science and Technology
Institute of Polymer Chemistry
College of Chemistry
Nankai University
Tianjin 300071, China

Prof. S. A. Ponomarenko
Chemistry Department
Moscow State University
Leninskie Gory 1–3, Moscow 119991, Russia

Prof. C. J. Brabec
Bavarian Center for Applied Energy Research (ZAE Bayern)
Haberstraße 2a, 91058 Erlangen, Germany

development of OPVs.[13,14] In order to exceed the threshold for OPVs' market success, these above-mentioned requirements need to be satisfied simultaneously. With the development of OPV science and technology, a general consensus among researchers about photovoltaic materials as a determinant factor is acceptable. Thus, amounts of structure–performance relationships and general guidelines for the material design were reported and highlighted.[15,16] Nevertheless, most academic research articles focusing on PCE only offer a partial answer to the question of whether a given material is suitable for OPV applications.[17–19] In fact, additional guidelines coming from the tight limitations set by industrial research and product development, and mainly including low cost and long-term stability, are hardly reported,[19–21] and generally cause some doubt and risks about the possible industrial future of OPV.

Different publications already investigated the cost analysis of an OPV technology.[22–24] And an acceptable cost, which leads to commercially viable OPV modules, is around 10 € g^{-1}.[24,25] The overall cost of an OPV module generally involves different contributions, including materials, capital costs, labor, and so on. A further cost analysis demonstrates that the overall costs depend primarily on the materials cost (including metal electrodes, buffer layers, active materials, solvents, etc.) even on a relatively small industrial scale, as high-yield printing and coating technologies do not suffer from high processing overheads.[24,25] Since the cost of the active material represents a significant part of the total, it suggests that synthetic accessibility of photovoltaic materials must be as low as possible to contribute to the possible industrial future of OPV. Generally, synthetic accessibility is proportional to its number of synthetic steps (NSS) and scalable purification processes.[19,26] Recently, Po et al. demonstrated that a preliminary indirect estimation of the cost of a photovoltaic material can be accomplished by considering its synthetic complexity (SC), assessed through five parameters (number of synthetic steps, reciprocal yield (RY), number of operation units for the isolation/purification (NUO), number of column chromatographies for the isolation/purification (NCC), and number of hazardous chemicals (NHC)).[18,21] This new SC factor not only predicts the actual contribution of molecular design but also provides a possibility whether one compound would clearly contribute to the OPV market success. In short, a complete evaluation of active materials should include an index related to the cost issue.

As mentioned above, OPVs have exceeded 11% efficiencies at research level, but to be commercially useful it is regularly stated that they must have lifetimes in excess of 10 years. Thus, achievement of long-term stability of organic photovoltaic is currently one of the major topics for this technology to reach maturity. Long-term stability of OPVs generally involves interface materials issues, degradation of photovoltaic materials, morphological stability of active layer, and physical encapsulation techniques.[27] With sufficient packaging to remove oxygen and moisture, it was found that some OPVs can be intrinsically stable under continuous photoexcitation, and degrade very little for over 4000 h.[28] Meanwhile, small organic photovoltaic modules on flexible substrates with operational lifetimes of a few years are available in the absence of oxygen and water.[28–30] These indirectly indicate that material photostability as well as their BHJ morphological stability resulting from its metastable nanostructure plays a vital role on the device stability. In material design, several factors, including the molecular structure of the backbone, the solubilizing side chain, molecular weight, material purity, etc., can have a strong impact on observed material and BHJ morphological stability.[15,20,27,31–33] For instance, McGehee and co-workers and Brabec and co-workers found that a high degree of crystallinity could significantly reduce the initial light-induced degradation, which is caused by light-induced traps.[34,35] We further found that the molecular structure attached various side chains as well as the morphological characteristics have a strong impact on the photostability in encapsulated devices.[20,36] In this case, although studying the photochemistry of photovoltaic materials will help elucidate the underlying chemical mechanisms and hopefully aid in material design, the key focus of stability should be on settings that are realistic in the context of production and end application. Thus, a standard text protocol (e.g., International Electrotechnical Commission (IEC) 61646 environmental chamber tests) for lifetime measurement for taking into consideration in the selection of an active material is desired to compare results measured the device photostability of organic materials under the real work environment.[37] Only thus can we suggest effective guidelines for the material design and evaluation.

The industrial commercialization and establishment of this photovoltaic technology into the market require a correct balanced among cost, stability, and efficiency, which are mainly determined by photovoltaic materials, thus a new strategy for material evaluation or material design in OPVs should be introduced to instead of the PCE factor. In the present study, we define an industrial figure of merit (i-FOM) for material applied accessibility containing three parameters: SC,[21] PCE, and device photostability. Thirty-five donor molecules are introduced to evaluate their SC with respect to the material cost. After that, device efficiencies optimized are provided, meanwhile maximum theoretical PCEs in single junction OPVs simulated by Scharber model and Baran's results are shown. Besides, device photostability indicating material performance is also measured under illumination in 200 h. The relationships between the mentioned key factors and the molecular structures based on 35 molecules are systematically analyzed, and some general guidelines for material design are provided. Combining with these investigations, 35 molecules are further ranked according to this i-FOM method. Overall, these results initiate a discussion re-reviewing the relevance of molecular structure as a powerful tool to optimize in parallel cost, device efficiency and photostability for OPV market success.

2. Results and Discussion

2.1. Method of Analysis and Data Handling

Combining with the above-mentioned analyses and the discussions in the introduction section, here we applied the three key factors, including SC, device efficiency and photostability, into the definition of a new i-FOM as described

$$\text{i-FOM} = \frac{\text{PCE} \times \text{photostability}}{\text{synthetic complexity}} \quad (1)$$

Here the photostability data are taking from a normal device under illumination and inert atmosphere. And the cost of active materials can be considered by their synthetic complexity. As expected, this i-FOM method can more precisely assess the accessibility of a given material used in potential OPV applications.

The molecular architectures of 35 investigated molecules, including star-shaped molecules SM1–SM13, 2D molecules SM14–SM17 and linear oligomers SM17–SM35, are listed in the **Scheme 1**. The synthesis routs of molecules SM1–SM35 with the exception of SM18, SM34, and SM35 are described in Scheme S1 (Supporting Information). The SC index of the molecules including SM18, SM34, and SM35 with their five parameters can be carried out from the literature.[21] The starting compounds for the molecular preparation were considered to be simpler chemical precursors that could be found on the market. Table S1 (Supporting Information) lists the five parameters defining the SC of the molecules. Besides, the bandgaps in eV and energy levels of all the molecules were determined from the optical absorption spectra of pristine films and estimated from the CV measurements, respectively, as summarized in **Table 1**.

The photovoltaic performance of molecules SM1–SM35, combined with [6,6]-phenyl-C71-butyric acid methyl ester ($PC_{70}BM$) acceptor, are optimized in our lab via a normal device architecture of ITO/PEDOT:PSS/active layers/Ca/Al. For each molecule, different PCE values are carried out through the use of optimized processing conditions described in the literatures and in the experimental section. In order to test the intrinsic stability of OSCs in a controlled environment and minimize extrinsic degradation through any uncertainty of package leaking, we constructed a portable environmental chamber that can hold devices at their maximum power point and simultaneously measure their current–voltage characteristics at fixed time intervals in a nitrogen atmosphere with less than 0.1 ppm water and oxygen. Note that we choose $PC_{70}BM$ as acceptor to reduce the photodimerization that occurs in [6,6]-phenyl-C61-butyric acid methyl ester (PCBM).[38] In addition, before loading the environmental chamber, current–voltage (I–V) curves of all devices with the expectation of SM18 were taken.

2.2. Synthesis Complexity

Figure 1 summarized the SC index of the various molecules discussed. Star-shaped molecules SM1–SM13 based on triphenylamine (TPA) as core on the left side present SC indexes of ≈40–62 because of the less number of synthetic steps, indicating the best possibilities of scaling up. Additionally, tri(2-methoxyphenyl)amine (TPA-MeO)-based star-shaped molecules including SM8–SM11 and SM13 generally exhibit the higher SC values as compared to TPA based molecule due to the slightly longer synthesis routes. Instead, 2D molecules SM14–SM17 based on benzo[1,2-b:4,5-b′]dithiophene (BDT) as central donor unit in the middle requires over ten synthetic steps, leading to SC indexes of 65–70. Those molecules would appear difficult to scale up at a reasonable cost. As compared to 2D molecules, linear molecule SM18 based on BDT unit require more synthesis and purification steps and thus show a low RY, which lead to a higher SC value of 81.5 among these BDT-based molecules. Linear oligomers SM19–SM30 show the SC values in the 70–83 regions, resulting from the multiple synthesis and purification steps of central units, which are comparable with the 2D molecules. Since the synthesis of linear molecule SM26 requires more synthesis and purification steps as well as increased number of hazardous chemicals, SM26 based on dithieno[3,2-b:2′,3′-d]silole (DTS) as a central unit and trithiophene as π-bridge shows the highest SC values of 82.9 among 35 molecules. Moreover, due to the different central units, the passage from SM31 to SM32 leads to a decrease of the SC index from 65 to 50, mainly resulting from the more difficult synthesis of thienothiadiazole (TT) unit as compared to benzothiadiazole (BT). This indicates the increase cost of mass producing TT-based molecules. Besides, both SM33 and SM34 showed the highest reported PCEs of ≈10%,[7] but reducing the π-bridge of SM34 to the shorter one SM33 results in a decrease of SC from 63.5 to 56.4. Importantly, the preparation of SM35 requires nine synthetic steps leading to a SC index of 50, although the large-scale synthesis of SM35 produces a side-product that cannot be easily separated.[39] Overall, the results presented demonstrate how the screening of 35 donor molecules for suitability in OPVs can be accomplished through rational synthesis.

2.3. Device Efficiencies

Typical performance data of prepared solar cells estimated from current density–voltage (J–V) characteristics are summarized in Table 1. Devices were processed following the recipes described in the relevant literatures and in the experimental section. Due to the use of Ca/Al electrodes and not further optimized layer thickness photovoltaic properties are slightly lower compared to best reported values. The solar cells based on star-shaped molecules SM1–SM13 showed the lower PCEs of ≈2%–4% as compared to the 2D molecule systems with the exception of SM14, mainly resulting from the low short-circuit current density (J_{sc}) and fill factor (FF) values. The photovoltaic performance of linear oligomers is hugely different as shown in Table 1, mainly due to different molecular structures and processing conditions. Although the bandgaps of oligomers SM19–SM30 are comparable with these of molecules SM33–SM35, they gave rather low J_{sc} and FF values (60%), thus limiting their PCEs to 6%. Interestingly, although SM31 and SM32 show the largely different optical bandgaps (E_g) due to the various central acceptor units, their device efficiencies are comparable, mainly resulting from their charge generation efficiencies and carrier transport properties.[39] Nevertheless, this trend is not in good agreement with the literature,[40] mainly contributed to the different processing technologies as described in the experimental section. Besides, the findings suggest that all investigated molecules suffer from typical open-circuit voltage (V_{oc}) losses, and all devices show typical ≥0.6 eV loss ($E_g - eV_{oc}$) in the device (see Figure S1 in the Supporting Information).

We adopted the optical simulation demonstrated by Scharber,[6] to tap the efficiency potential of these molecules. Based on the reviews of high-performance single-junction solar cells,[5,41,42] a FF of 75% and an average external quantum efficiencies (EQE) of 75% are assumed in this study. As a result,

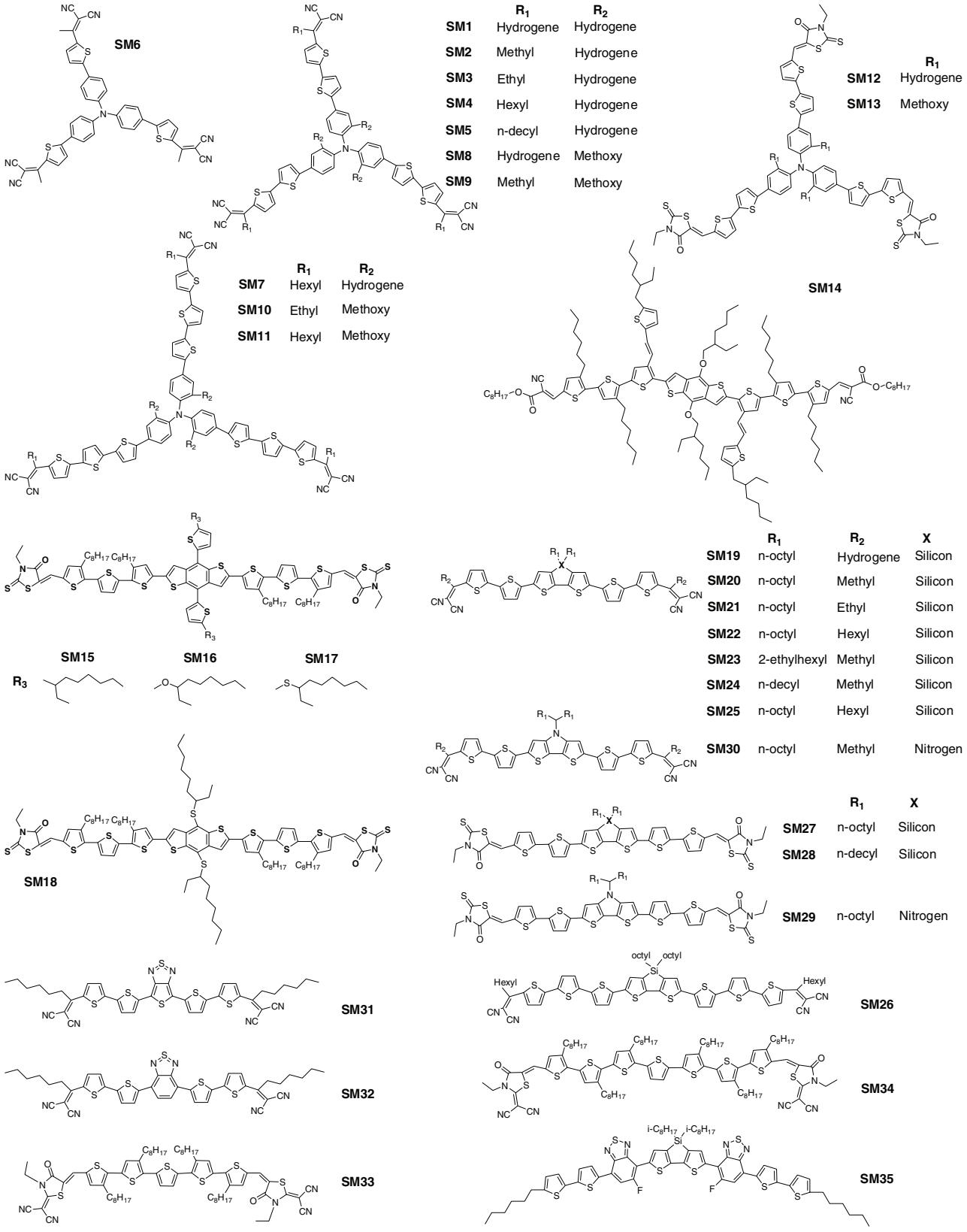

Scheme 1. Chemical structures of the investigated molecules SM1–SM35.

Table 1. Combination sheet for donors and acceptors in the screening. (1) The optical bandgap in eV estimated from the absorption spectrum. (2) The value of the HOMO and LUMO energy levels estimated from the CV measurements, both in eV. (3) Values of the reported V_{oc} are measured under one sun illumination. (4) Values of the E_g loss ($E_g - V_{oc}$). (5) The reported PCEs tested under one sun.

Compd.	Small molecules	Bandgaps [eV][a)]	HOMO/LUMO levels[a)]	V_{oc} [V][b)]	E_g–loss	PCE [%][b)]	Refs.
SM1	N(Ph-2T-DCV)$_3$	1.78	–5.17/–3.39	0.92	0.86	2.07	[55]
SM2	N(Ph-2T-DCV-Me)$_3$	1.80	–5.32/–3.41	0.98	0.82	4.95	[56]
SM3	N(Ph-2T-DCV-Et)$_3$	1.92	–5.32/–3.40	0.96	0.96	3.65	[56]
SM4	N(Ph-2T-DCV-Hex)$_3$	1.95	–5.34/–3.41	0.98	0.97	3.33	[56]
SM5	N(Ph-2T-DCV-Dodec)$_3$	1.93	–5.34/–3.40	1.00	0.93	2.96	[56]
SM6	N(Ph-1T-DCV-Me)$_3$	2.08	–5.60/–3.46	1.06	1.02	2.42	[55]
SM7	N(Ph-3T-DCV-Hex)$_3$	1.85	–5.26/–3.40	0.92	0.93	4.04	[57]
SM8	N(Ph(OMe)-2T-DCV)$_3$	1.75	–5.20/–3.46	0.90	0.85	3.54	[58]
SM9	N(Ph(OMe)-2T-DCV-Me)$_3$	1.80	–5.20/–3.38	0.92	0.88	4.21	[58]
SM10	N(Ph(OMe)-3T-DCV-Et)$_3$	1.80	–5.14/–3.37	0.82	0.98	3.23	[58]
SM11	N(Ph(OMe)-3T-DCV-Hex)$_3$	1.80	–5.14/–3.37	0.86	0.94	3.03	[58]
SM12	N(Ph-2T-Rh-Et)$_3$	1.77	–5.30/–3.42	0.95	0.82	3.86	[59]
SM13	N(Ph(OMe)-2T-Rh-Et)$_3$	1.68	–5.22/–3.38	0.91	0.77	3.78	[59]
SM14	DCA3T(VT)BDT	1.83	–5.33/–3.44	0.92	0.91	3.84	[60]
SM15	BDTT-TR	1.74	–5.17/–3.39	0.93	0.81	7.44	[20]
SM16	BDTT-O-TR	1.74	–5.14/–3.34	0.90	0.84	6.50	[20]
SM17	BDTT-S-TR	1.73	–5.18/–3.25	0.97	0.76	9.20	[20]
SM18	DR3TSBDT[c)]	1.74	–5.07/–3.33	0.91	0.83	9.95[c)]	[42]
SM19	DTS(Oct)$_2$-(2T-DCV)$_2$	1.65	–5.32/–3.45	0.84	0.81	1.50	[61]
SM20	DTS(Oct)$_2$-(2T-DCV-Me)$_2$	1.60	–5.26/–3.34	0.90	0.70	5.91	[61]
SM21	DTS(Oct)$_2$-(2T-DCV-Et)$_2$	1.62	–5.32/–3.39	0.90	0.72	4.20	[61]
SM22	DTS(Oct)$_2$-(2T-DCV-Hex)$_2$	1.72	–5.30/–3.35	0.95	0.76	1.80	[61]
SM23	DTS(EtHex)$_2$-(2T-DCV-Me)$_2$	1.64	–5.32/–3.39	0.90	0.74	4.10	[61]
SM24	DTS(Dec)$_2$-(2T-DCV-Me)$_2$	1.64	–5.32/–3.37	0.90	0.74	4.60	[61]
SM25	CPDT(Oct)$_2$-(2T-DCV-Hex)$_2$	1.60	–5.29/–3.34	0.91	0.69	2.34	[62]
SM26	DTS(Oct)$_2$-(3T-DCV-Hex)$_2$	1.65	–5.16/–3.27	0.79	0.86	2.29	[62]
SM27	DTS(Oct)$_2$-(2T-Rh-Et)$_2$	1.62	–5.22/–3.33	0.84	0.78	4.80	[63]
SM28	DTP(Dec)$_2$-(2T-Rh-Et)$_2$	1.53	–5.20/–3.40	0.82	0.71	4.27	[63]
SM29	DTP(Oct)$_2$-(2T-Rh-Et)$_2$	1.53	–5.08/–3.35	0.75	0.78	3.16	[63]
SM30	DTP(Oct)$_2$-(2T-DCV-Me)$_2$	1.45	–5.09/–3.40	0.70	0.75	5.13	[63]
SM31	TT-(2T-DCV-Hex)$_2$	1.25	–5.11/–3.46	0.64	0.61	1.32	[40]
SM32	BT-(2T-DCV-Hex)$_2$	1.72	–5.55/–3.45	1.03	0.69	1.67	[40]
SM33	DRCN5T	1.60	–5.22/–3.41	0.93	0.67	8.97	[7]
SM34	DRCN7T	1.62	–5.08/–3.44	0.92	0.70	8.62	[7]
SM35	T1	1.50	–5.20/–3.60	0.78	0.72	6.91	[64]

[a)]Data from the cited references (right column); [b)]Data from the investigated solar cells with a device architecture of ITO/PEDOT:PSS/active layers/Ca/Al; [c)]Data from the ref. [41] with an ETL-1/Al as cathode.

the outcome of the optical simulation and the theoretical PCEs of the corresponding devices as a function materials' bandgap are represented in **Figure 2**a. In the contour plot, the PCE is plotted versus the absorption onset and the HOMO position of the donor. With a minimum lowest unoccupied molecular orbit Δ(LUMO) of 0.3 eV,[6] a maximum efficiency of over 13% is achievable for BHJ devices based on a donor material with an optimum bandgap of 1.45 eV. One can be found that several molecules treated by optimization methods do have a performance potential over 10% PCE. It must be noted that the LUMO level of PCBM is assumed to be –4.3 eV. Actually, some groups report different values for this parameter, due to variation in experimental protocols of measurements. Therefore, for some compounds (namely, SM33–35) estimated maximum theoretical PCEs are lower than experimental ones. In these cases, i-FOMs were calculated with the latter values.

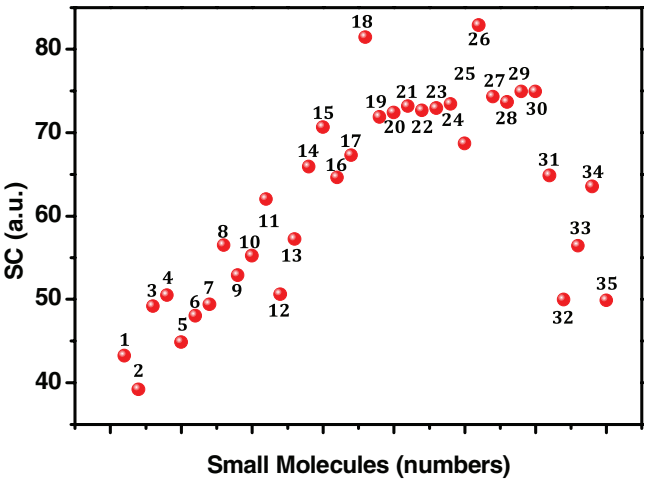

Figure 1. SC index of the investigated small molecules.

Recently, a lot of efforts have been made in the past few years to develop the next-generation nonfullerene acceptors (NFAs) for OPVs.[5,43–45] Many fullerene-free devices with the PCEs of over 9% were reported with higher V_{oc} and minor energy level offset between donor and acceptor (D/A), i.e., ΔE_{LUMO} and/or ΔE_{HOMO} values is less than the widely acknowledged 0.3 eV energy needed for dissociating the tightly bound Frenkel excitons to produce spatially separated changes.[46–48] It suggests that the LUMO level offsets in OPVs always overestimate the energy requires for charge separation and the offsets must not be required.[49–52] In other words, V_{oc} can be tuned more efficiently considering that it is proportional to the band gap of the donor materials as described here $\left(V_{oc} = \frac{1}{e} E_g^{Donor} - 0.6\right)$.[1,53] Recently, Baran et al. reported that the empirical limit can be overcome using NFAs blended with a low bandgap polymer PffBT4T-2DT leading to efficiencies approaching 10%. Importantly, a V_{oc} up to 1.12 V, which corresponding to a loss of only $E_g/_q - V_{oc} = 0.5$ V,[54] was found in this system. Based on the investigations and results, here we can further described an Equation (2) for PCE evaluation,

$$V_{oc} \approx \frac{1}{e} E_g^{BHJ} - 0.5V \quad (2)$$

Here E_g^{BHJ} is the optical band gap of the BHJ blend films for efficiency evaluation. And the E_g^{BHJ} value depends on the optical bandgap of donor or acceptor, which shows the broader absorption spectra in film. Thus, we put forward a summary estimate of ultimate device efficiency that can be derived as a function of the bandgap of BHJ blend (see Figure 2b). We find PCE over 14% for E_g^{BHJ} 1.17–1.57 eV (790–1060 nm) when we assume a constant EQE = 75% and a FF = 75%. As expected, the values for the best cells based on all the molecules SM1–SM35 can approach this maximum theoretical efficiency if the novel and suitable acceptor materials with improved electrical and optical properties are introduced.

2.4. Device Stability

In order to effectively evaluate photovoltaic materials, in this study we directly introduced a test protocol for lifetime measurement, which is desired to indirectly but clearly compare the device photostability of various systems recorded in standard conditions. The main goals of this protocol are to provide real guidelines for designing next generation photovoltaic materials for thermally and photostable solar cells. **Figure 3** illustrates the variation of normalized average PCE losses for the encapsulated devices. The detailed losses of photovoltaic parameters with the exception of SM18 are shown in Figures S2–S35 (Supporting Information), which also contains the photoluminescence (PL) spectra of pristine films before and after about 200 h under one sun illumination.

Although degradation processes of each system are still not fully understood,[32] several guidelines with the respect to the relationships between molecular structure and their

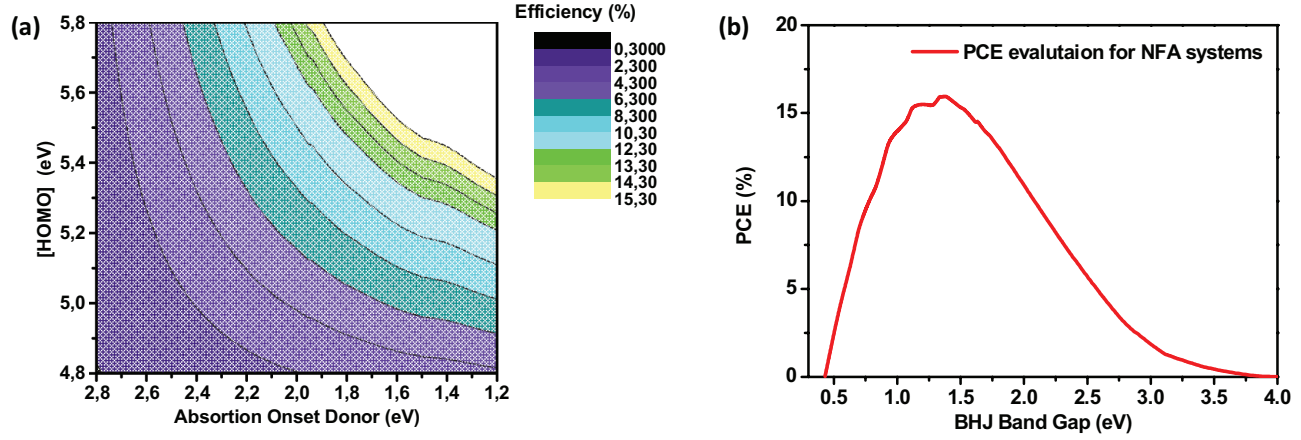

Figure 2. a) Contour plot showing the calculated PCE (contour lines and colors) versus the absorption onset and the HOMO level of the donor material according to ref. [1] assuming an EQE, a FF of 75% and V_{oc} according to Equation $\left(V_{oc} = \frac{1}{e}(E_{HOMO}^{D} - E_{LUMO}^{PCBM}) - 0.3V\right)$ was used. For the calculation, the used LUMO level of PCBM is 4.3 eV. b) Theoretical efficiency of BHJ photovoltaic devices with $E_g - eV_{oc} = 0.5$ eV versus the lowest optical band gap of the BHJ blend films, calculated using the AM 1.5 spectrum. For the calculation an EQE of 75% and a FF of 75% were used.[54]

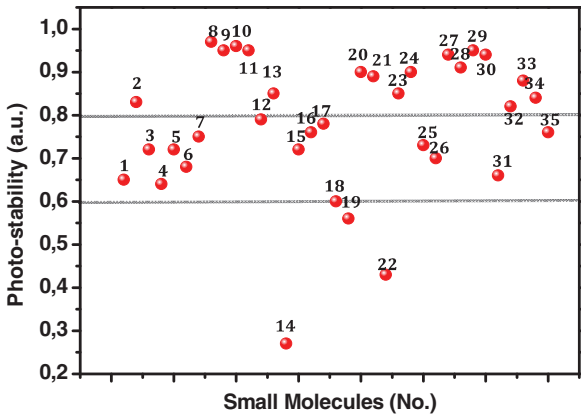

Figure 3. Variation of normalized average PCE losses over illumination time for the encapsulated devices based on molecules SM1–SM35.

photostability have been identified. The device photostability was found to be higher for star-shaped molecules with the tris(2-methoxyphenyl)amine (m-TPA) donor unit as a central core (SM8–SM11 and SM13), as compared to the TPA-based molecules (SM1–SM7 and SM12), indicating m-TPA unit is more stable donor monomer. Among the 2D molecules, SM14 with central alkoxy-substituted BDT unit exhibited the poorest photostability than the other molecules with alkyl-substituted BDT units. The photovoltaic performance of SM14 decreased to 27% of the initial efficiency after illumination while other 2D molecules decreased to only 30%–40% PCE loss. This result is good agreement with the literatures,[65,66] where alkyl-substituted BDT unit were reported to be the poor stable unit in relevant polymers. Furthermore, this trend is confirmed by the changes in PL intensity, i.e., $\Delta I = (I_t - I_0)/I_0$, where I_0 and I_t are the PL intensities before and after degradation, respectively.[28,29] As shown in Figure S36 (Supporting Information), SM14 showed the higher ΔI value of 0.45, indicating the poor photostability in the pristine film. It directly resulted in the worse long-term stability in devices. In addition, terminal dicyanovinyl (DCV) acceptor units without (SM1 and SM19) and with long alkyl side chains (SM5, SM22, and SM25) are the most susceptible to degradation and impart low device photostability. And gaining ΔI values of these molecules are more accelerated than the other relevant molecules (SM21 and SM 22, see Figure S36 in the Supporting Information). Finally, SM33 and SM34 device, which exhibited the recorded PCEs in the literature,[7,67] showed light-induced losses to ≈88% and 84% within 200 h, respectively, while SM35 lost significantly lost ≈76% over the same period. Importantly, among the oligomers, SM19 and SM22 showed the weaker photostability. The ΔI changes of pristine films, however, are not in consistent with their degradation of PCEs, probably contributed to the other intrinsic degradation mechanisms caused in devices (e.g., morphological changes and light-indcued fullerene dimerization).[67–69] Combining with these results and analyses, it is worth noting that the effect of molecular engineering on the stability of OPVs is certainly more subtle than originally expected and is recommended for more in-depth investigations to develop better detailed molecular insight on the changes of material structure and blend morphology during degradation and hopefully aid in material design.

2.5. Industrial Figure of Merit

Based on the main factors as discussed above, the defined i-FOM can be considered a rough, but reasonable, tool to evaluate the accessibility of photovoltaic materials used in possible OPV applications, and best represents the cost-efficiency-stability balance of a given donor material. Figure S37 (Supporting Information) shows a plot of the device efficiency and photostability of molecules SM1–SM35 versus their synthetic complexity. In general, regions with the high i-FOM values correspond to small molecules with relatively high device efficiency and photostability as well as fair accessibility. Nevertheless, we should further put three different thresholds with respect to SC, PCE, and photostability for OPV's market success: the investigated molecules, whose SCs of over 80, PCEs of below 4%, and photostability values of below 80%, respectively, are not suitable for commercial applications. Thus, in order to precisely evaluate molecule performance and provide reasonable design strategies, we should kick out these uncomfortable molecules. For instance, SM17 and SM35 exhibited the high i-FOM values of over 10%, but their photostability of below 80% is not suitable for further application. Besides, SM18 has the highest PCE (close to 10%) among these molecules,[42] but its SC exceed 80, resulting in a low i-FOM value (7.3%), which is also not suitable for market success. As a result, **Figure 4** shows the molecules whose performance passes these thresholds. Only three molecules, including star-shaped molecule SM2 and oligomers SM33 (DRCN5T) and SM34 (DRCN7T), offer the best trade-off with the i-FOM values of over 10%. SM2 shows the lowest SC value of below 40%, but the device efficiency (a PCE of around 5%) and photostability (a degradation value of 83%) are not remarkable. SM33 and SM34 are even more complex for molecular synthesis, although they possess high PCEs closing to 9% and comparable photostability values (84% and 88%, respectively). Importantly, SM33 as a widely studied oligomer (DRCN5T) has the highest i-FOM value (14%), mainly resulting from its simple preparation and high PCE. This result makes this molecule structure the most suitable one for highly efficient and scalable OPV.

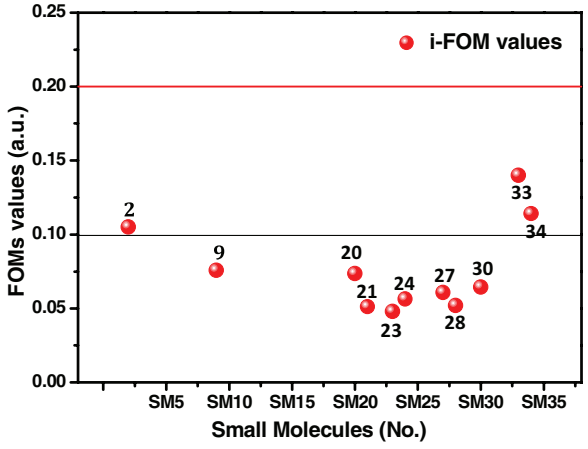

Figure 4. i-FOM of molecules whose performance exceed these thresholds, the red line as a maximum theoretical i-FOM value defined.

In order to evaluate the possibilities of molecular donor materials for achieving the requirements for commercial applications, a maximum theoretical i-FOM need to be defined. Considering a widespread development of OPVs as large-area, roof-top applications for residential and commercial buildings, high module efficiencies >10% and lifetimes >10 years are required.[70] Thus, we can define an idea photovoltaic material with a PCE of 10% and a neglectful performance degradation under constant illumination. Viewing the literatures,[5,71] the highest reported PCEs are mostly obtained with these more complex donor materials. This general trend is also demonstrated in fullerene-based systems by us and Po et al.[21] We found that the PCEs of over 9% generally show the SC values of over 50%. It is clear to note that the SCs of donor and acceptor materials in fullerene-free OPVs must be considered together. Thus, a higher SC for the evaluation of nonfullerene systems is foreseeable. Reviewing these issues, a SC of around 50% is needed for evaluation of applied materials and/or systems in devices. Therefore, a maximum theoretical i-FOM of 20% (a red line in Figure 4) is sufficient, clearly underlining the need to develop new photovoltaic materials and thus reduce the trade-off distance. Besides, a complete analysis and evaluation of active materials should also include an index related to the material processability, which is not available to record so far.[18] Further systematic studies are encouraged to give a more complete picture.

3. Conclusion

Thirty-five light-absorbing molecules are introduced to assess their material properties in OPVs via a new evaluation strategy containing three parameters: synthetic complexity, device efficiency, and photostability. The SC analysis demonstrated that the molecular backbone can significantly influence the SC, but not the side chains. Moreover, the molecules with more complex molecular architectures generally show the better PCEs. In addition, combining with $PC_{70}BM$ as acceptor, we applied a normal device structure to gain the optimized device efficiencies based on these molecules. Furthermore, we adopted the optical simulation demonstrated by Scharber and Baran's results, respectively, to tap the efficiency potential of the molecules. The PCEs as expected for some investigated molecules can approach the maximum theoretical efficiencies if suitable acceptors with improved electrical and optical properties are applied. Except the device efficiencies, the materials offering device photostability are also identified, meanwhile some guidelines for the future research on high-performance photovoltaic materials are presented. As a final survey, an i-FOM method is introduced to analysis the properties of investigated molecules and predict their possible industrial future of OPV. Among these molecules, SM33 (DRCN5T) shows the highest i-FOM value (14%), although it is still far from achieving the commercial requirements of OPVs, corresponding to a theoretical optimization i-FOM value of 20%. In short, our work demonstrates the challenges associated with the material design for OPV applications, which contains a multitude of factors and progress obviously beyond simple criteria such as evaluation according to PCE alone. Our i-FOM approach as a powerful tool can provide valuable insights for those attempting to realize the efficient evaluation of photovoltaic materials.

4. Experimental Section

Materials: The BHJ donor materials under this study are molecules SM1–SM35. SM1–SM13 and SM19–SM32 were provided by Prof. Sergei A. Ponomarenko. SM14–SM17 were provided by Dr. Chaohua Cui and Prof. Yongfang Li. SM33 and SM34 were provided by Prof. Yongsheng Chen. SM35 was purchased from Luminescence Technology Corp (Hsin-Chu, Taiwan). $PC_{70}BM$ was purchased from Nano-C (Westwood, MA, USA). The optical bandgap and CV data of investigated materials can be found in the literatures listed in Table 1. Other starting materials were used as purchased from commercial sources unless stated otherwise.

Device Fabrication: All of conventional photovoltaic devices were processed and characterized in ambient atmosphere. Prestructured ITO-coated glass substrates (as obtained from Osram) were subsequently cleaned in acetone and isopropyl alcohol for 10 min each. After drying, the substrates were bladed with 30 nm PEDOT:PSS (Heraeus, Clevios P VP. Al 4083). The SM1–SM13 bulk films (≈60–80 nm) was doctor bladed in ambient air from the relevant solutions (optimal D/A ratios; 10 mg mL^{-1}) in dichlorobenzene without any other processes. The SM14–SM35 blend films (≈100 nm) were spin-coated in ambient air from the relevant solutions (optimal D/A ratios; 15 mg mL^{-1}) in chloroform. The detailed processing conditions can be found in the relative literatures.[17,20,37,60–62,72] Note that SM31 and SM32 here were spin-coated on the top of PEDOT:PSS layer, which is different with our previous experiments.[40] Some active layers (e.g., SM33 and SM34) were further processed with various post-treatment conditions. More details about the fabrications of BHJ blends can be found in relevant references. After that, the annealed samples were removed to the glovebox for evaporating cathodes. For solar cell 15 nm Ca and 100 nm Al were thermally evaporated at a base pressure below 10^{-6} mbar through shadow masks to form an active area of 10.4 mm^2. The current–voltage characteristics of the solar cells were measured under AM 1.5 G irradiation of an OrielSol1A Solar simulator (100 mW cm^{-2}). The light source was calibrated by using a silicon reference cell. The reported PCE data are average values over the six devices of each sample. PL data were collected using a Perkin-Elmer LS55 Fluorescence Spectrometer. The PL excitation wavelength was set to 455 nm.

Light-Induced Degradation Testing: We performed light-induced degradation experiments with one sun equivalent illumination intensity for ≈200 h on investigated molecules investigated. The solar cells were fabricated in a glovebox and were loaded into an aluminum chamber with a glass from plate, and further aged under high vacuum, excluding the well-known effects of oxygen degradation from our experiments. The atmosphere chamber was vented into the lab via a check valve. The gas flow in and out of the camber through copper pipes was kept continuous throughout the experiment. It is important to operate all devices at temperatures below their solid–liquid transition temperature to avoid thermally induced morphological changes. In addition, we minimized the thermal degradation by using white light LED's. The investigated solar cells were built in a standard device architecture with PEDOT:PSS and calcium–aluminum contacts. Current–voltage characteristics were recorded using a Keithley 2400 source meter. The aging apparatus operated through a LabVIEW interface that dynamically held each solar cell at maximum power point and graphically recorded the current–voltage curve every 30 min for all testing duration. Each solar cell in this study with the exception of SM18-based device followed an optimal layer combination and fabrication procedure to yield the highest PCE (Table 1). There were at least six different solar cells for each type of SM BHJ in the test. Table S2 (Supporting Information) shows the average photostability data of the each type of SM BHJ, which was stop being monitored after 200 h.

Supporting Information

Supporting Information is available from the Wiley Online Library or from the author.

Acknowledgements

The authors gratefully acknowledge the support of the Cluster of Excellence ''Engineering of Advanced Materials'' at the University of Erlangen-Nuremberg, which was funded by the German Research Foundation (DFG) within the framework of its ''Excellence Initiative.'' The work was also partially funded by the Sonderforschungsbereich 953 "Synthetic Carbon Allotropes." The authors also thank the support of "Solar Technologies go Hybrid" (SolTech) project and the Energy Campus Nürnberg (EnCN) financed by the Bavarian state government. J.M. acknowledge funding from Wuhan University. C.C. and Y.L. acknowledge funding from Jiangsu Provincial Natural Science Foundation (Grant No. BK20150327), NSFC (No. 91333204), Natural Science Foundation of the Jiangsu Higher Education Institutions of China (Grant No. 15KJB430028), and Project Funded by China Postdoctoral Science Foundation (Grant No. 2015M581855). Y.N.L. and S.A.P. acknowledge financial support from the Russian Science Foundation (grant No. 14-13-01380). Y.N.L. acknowledges also the Russian Foundation for Basic Research (grant No. 15-33-20957). B.K., X.W., and Y.C. acknowledge funding from MoST (Grant No. 2014CB643502).

Conflict of Interest

The authors declare no conflict of interest.

Keywords

industrial figure of merit, long-term stability, low cost, power conversion efficiency, processability

Received: February 21, 2017
Revised: March 29, 2017
Published online:

[1] M. C. Scharber, N. S. Sariciftci, *Prog. Polym. Sci.* **2013**, *38*, 1929.
[2] C. J. Brabec, S. Gowrisanker, J. J. M. Halls, D. Laird, S. Jia, S. P. Williams, *Adv. Mater.* **2010**, *22*, 3839.
[3] L. Lu, T. Zheng, Q. Wu, A. M. Schneider, D. Zhao, L. Yu, *Chem. Rev.* **2015**, *115*, 6854.
[4] J. Min, Z. Zhang, C. Cui, Y. N. Luponosov, I. Ata, P. Schweizer, T. Przybilla, F. Guo, T. Ameri, K. Forberich, E. Spiecker, P. Bäuerle, S. A. Ponomarenko, Y. Li, C. J. Brabec, *Adv. Funct. Mater.* **2016**, *26*, 4543.
[5] S. Zhang, L. Ye, J. Hou, *Adv. Energy Mater.* **2016**, *6*, 1502529.
[6] M. C. Scharber, *Adv. Mater.* **2016**, *28*, 1994.
[7] B. Kan, M. Li, Q. Zhang, F. Liu, X. Wan, Y. Wang, W. Ni, G. Long, X. Yang, H. Feng, Y. Zuo, M. Zhang, F. Huang, Y. Cao, T. P. Russell, Y. Chen, *J. Am. Chem. Soc.* **2015**, *137*, 3886.
[8] H. Bin, L. Gao, Z. G. Zhang, Y. Yang, Y. Zhang, C. Zhang, S. Chen, L. Xue, C. Yang, M. Xiao, Y. Li, *Nat. Commun.* **2016**, *7*, 13651.
[9] Z. Zheng, O. M. Awartani, B. Gautam, D. Liu, Y. Qin, W. Li, A. Bataller, K. Gundogdu, H. Ade, J. Hou, *Adv. Mater.* **2017**, *29*, 1604241.
[10] D. J. Burke, D. J. Lipomi, *Energy Environ. Sci.* **2013**, *6*, 2053.
[11] M. Helgesen, J. E. Carlé, F. C. Krebs, *Adv. Energy Mater.* **2013**, *3*, 1664.
[12] T. R. Andersen, H. F. Dam, B. Andreasen, M. Hösel, M. V. Madsen, S. A. Gevorgyan, R. R. Søndergaard, M. Jørgensen, F. C. Krebs, *Sol. Energy Mater. Sol. Cells* **2014**, *120*, 735.
[13] R. Po, A. Bernardi, A. Calabrese, C. Carbonera, G. Corso, A. Pellegrino, *Energy Environ. Sci.* **2014**, *7*, 925.
[14] F. C. Krebs, *Sol. Energy Mater. Sol. Cells* **2009**, *93*, 394.
[15] L. Lu, T. Zheng, Q. Wu, A. M. Schneider, D. Zhao, L. Yu, *Chem. Rev.* **2015**, *115*, 12666.
[16] S. Zhang, L. Ye, W. Zhao, B. Yang, Q. Wang, J. Hou, *Sci. China Chem.* **2015**, *58*, 248.
[17] C. Cui, X. Guo, J. Min, B. Guo, X. Cheng, M. Zhang, C. J. Brabec, Y. Li, *Adv Mater.* **2015**, *27*, 7469.
[18] R. Po, G. Bianchi, C. Carbonera, A. Pellegrino, *Macromolecules* **2015**, *48*, 453.
[19] E. Bundgaard, F. Livi, O. Hagemann, J. E. Carlé, M. Helgesen, I. M. Heckler, N. K. Zawacka, D. Angmo, T. T. Larsen-Olsen, G. A. dos Reis Benatto, B. Roth, M. V. Madsen, M. R. Andersson, M. Jørgensen, R. R. Søndergaard, F. C. Krebs, *Adv. Energy Mater.* **2015**, *5*, 1402186.
[20] J. Min, C. Cui, T. Heumueller, S. Fladischer, X. Cheng, E. Spiecker, Y. Li, C. J. Brabec, *Adv. Energy Mater.* **2016**, *6*, 1600515.
[21] R. Po, J. Roncali, *J. Mater. Chem. C* **2016**, *4*, 3677.
[22] J. Kalowekamo, E. Baker, *Sol. Energy* **2009**, *83*, 1224.
[23] B. Azzopardi, C. J. M. Emmott, A. Urbina, F. C. Krebs, J. Mutale, J. Nelson, *Energy Environ. Sci.* **2011**, *4*, 3741.
[24] F. Machui, M. Hosel, N. Li, G. D. Spyropoulos, T. Ameri, R. R. Sondergaard, M. Jorgensen, A. Scheel, D. Gaiser, K. Kreul, D. Lenssen, M. Legros, N. Lemaitre, M. Vilkman, M. Valimaki, S. Nordman, C. J. Brabec, F. C. Krebs, *Energy Environ. Sci.* **2014**, *7*, 2792.
[25] L. Lucera, P. Kubis, F. W. Fecher, C. Bronnbauer, M. Turbiez, K. Forberich, T. Ameri, H. Egelhaaf, C. J. Brabec, *Energy Technol.* **2015**, *3*, 373.
[26] N. Espinosa, R. García-Valverde, A. Urbina, F. Lenzmann, M. Manceau, D. Angmo, F. C. Krebs, *Sol. Energy Mater. Sol. Cells* **2012**, *97*, 3.
[27] P. Cheng, X. Zhan, *Chem. Soc. Rev.* **2016**, *45*, 2544.
[28] W. R. Mateker, I. T. Sachs-Quintana, G. F. Burkhard, R. Cheacharoen, M. D. McGehee, *Chem. Mater.* **2015**, *27*, 404.
[29] J. A. Hauch, P. Schilinsky, S. A. Choulis, S. Rajoelson, C. J. Brabec, *Appl. Phys. Lett.* **2008**, *93*, 103306.
[30] S. B. Sapkota, A. Spies, B. Zimmermann, I. Dürr, U. Würfel, *Sol. Energy Mater. Sol. Cells* **2014**, *130*, 144.
[31] W. R. Mateker, T. Heumueller, R. Cheacharoen, I. T. Sachs-Quintana, M. D. McGehee, J. Warnan, P. M. Beaujuge, X. Liu, G. C. Bazan, *Chem. Mater.* **2015**, *27*, 6345.
[32] M. Jørgensen, K. Norrman, F. C. Krebs, *Sol. Energy Mater. Sol. Cells* **2008**, *92*, 686.
[33] T. Heumueller, W. R. Mateker, A. Distler, U. F. Fritze, R. Cheacharoen, W. H. Nguyen, M. Biele, M. Salvador, M. von Delius, H.-J. Egelhaaf, M. D. McGehee, C. J. Brabec, *Energy Environ. Sci.* **2016**, *9*, 247.
[34] T. Heumueller, W. R. Mateker, I. T. Sachs-Quintana, K. Vandewal, J. A. Bartelt, T. M. Burke, T. Ameri, C. J. Brabec, M. D. McGehee, *Energy Environ. Sci.* **2014**, *7*, 2974.
[35] T. Heumueller, T. M. Burke, W. R. Mateker, I. T. Sachs-Quintana, K. Vandewal, C. J. Brabec, M. D. McGehee, *Adv. Energy Mater.* **2015**, *5*, 1500111.
[36] J. Min, X. Jiao, V. Sgobba, B. Kan, T. Heumüller, S. Rechberger, E. Spiecker, D. M. Guldi, X. Wan, Y. Chen, H. Ade, C. J. Brabec, *Nano Energy* **2016**, *28*, 241.
[37] F. Yan, J. Noble, J. Peltola, S. Wicks, S. Balasubramanian, *Sol. Energy Mater. Sol. Cells* **2013**, *114*, 214.
[38] a) T. M. Clarke, C. Lungenschmied, J. Peet, N. Drolet, K. Sunahara, A. Furube, A. J. Mozer, *Adv. Energy Mater.* **2013**, *3*, 1473. b) I. F. Domínguez, A. Distler, L. Lüer, *Adv. Energy Mater.* **2016**, *6*, 1601320.

[39] W. L. Leong, G. C. Welch, L. G. Kaake, C. J. Takacs, Y. Sun, G. C. Bazan, A. J. Heeger, *Chem. Sci.* **2012**, *3*, 2103.
[40] Y. N. Luponosov, J. Min, D. A. Khanin, D. Baran, S. A. Pisarev, S. M. Peregudova, P. V. Dmitryakov, S. N. Chvalun, G. V. Cherkaev, E. A. Svidchenko, T. Ameri, C. J. Brabec, S. A. Ponomarenkoa, *J. Photonics Energy* **2015**, *5*, 057213.
[41] K. Sun, Z. Xiao, S. Lu, W. Zajaczkowski, W. Pisula, E. Hanssen, J. M. White, R. M. Williamson, J. Subbiah, J. Ouyang, A. B. Holmes, W. W. Wong, D. J. Jones, *Nat. Commun.* **2015**, *6*, 6013.
[42] B. Kan, Q. Zhang, M. Li, X. Wan, W. Ni, G. Long, Y. Wang, X. Yang, H. Feng, Y. Chen, *J. Am. Chem. Soc.* **2014**, *136*, 15529.
[43] G. Sauve, R. Fernando, *J. Phys. Chem. Lett.* **2015**, *6*, 3770.
[44] C. B. Nielsen, S. Holliday, H. Y. Chen, S. J. Cryer, I. McCulloch, *Acc. Chem. Res.* **2015**, *48*, 2803.
[45] S. M. McAfee, J. M. Topple, I. G. Hill, G. C. Welch, *J. Mater. Chem. A* **2015**, *3*, 16393.
[46] W. Zhao, D. Qian, S. Zhang, S. Li, O. Inganas, F. Gao, J. Hou, *Adv. Mater.* **2016**, *28*, 4734.
[47] H. Bin, Z. G. Zhang, L. Gao, S. Chen, L. Zhong, L. Xue, C. Yang, Y. Li, *J. Am. Chem. Soc.* **2016**, *138*, 4657.
[48] Y. Lin, F. Zhao, Q. He, L. Huo, Y. Wu, T. C. Parker, W. Ma, Y. Sun, C. Wang, D. Zhu, A. J. Heeger, S. R. Marder, X. Zhan, *J. Am. Chem. Soc.* **2016**, *138*, 4955.
[49] X. Gong, M. Tong, F. G. Brunetti, J. Seo, Y. Sun, D. Moses, F. Wudl, A. J. Heeger, *Adv. Mater.* **2011**, *23*, 2272.
[50] K. Zhao, Q. Wang, B. Xu, W. Zhao, X. Liu, B. Yang, M. Sun, J. Hou, *J. Mater. Chem. A* **2016**, *4*, 9511.
[51] H. Zhang, S. Li, B. Xu, H. Yao, B. Yang, J. Hou, *J. Mater. Chem. A* **2016**, *4*, 18043.
[52] S. V. Gupta, A. Bagui, S. P. Singh, *Adv. Funct. Mater.* **2017**, *27*, 1603820.
[53] N. Li, D. Baran, K. Forberich, F. Machui, T. Ameri, M. Turbiez, M. Carrasco-Orozco, M. Drees, A. Facchetti, F. C. Krebs, C. J. Brabec, *Energy Environ. Sci.* **2013**, *6*, 3407.
[54] D. Baran, T. Kirchartz, S. Wheeler, S. Dimitrov, M. Abdelsamie, J. Gorman, R. Ashraf, S. Holliday, A. Wadsworth, N. Gasparini, P. Kaienburg, H. Yan, A. Amassian, C. J. Brabec, J. Durrant, I. McCulloch, *Energy Environ. Sci.* **2016**, *9*, 3783.
[55] S. A. Ponomarenko, Y. N. Luponosov, J. Min, A. N. Solodukhin, N. M. Surin, M. A. Shcherbina, S. N. Chvalun, T. Ameri, C. Brabec, *Faraday Discuss.* **2014**, *174*, 313.
[56] J. Min, Y. N. Luponosov, A. Gerl, M. S. Polinskaya, S. M. Peregudova, P. V. Dmitryakov, A. V. Bakirov, M. A. Shcherbina, S. N. Chvalun, S. Grigorian, N. Kaush-Busies, S. A. Ponomarenko, T. Ameri, C. J. Brabec, *Adv. Energy Mater.* **2014**, *4*, 1301234.
[57] J. Min, Y. N. Luponosov, D. Baran, S. N. Chvalun, M. A. Shcherbina, A. V. Bakirov, P. V. Dmitryakov, S. M. Peregudova, N. Kausch-Busies, S. A. Ponomarenko, T. Ameri, C. J. Brabec, *J. Mater. Chem. A* **2014**, *2*, 16135.
[58] Y. Luponosov, M. Jie, A. N. Solodukhin, A. V. Bakirov, P. v. Dmitryakov, M. A. Shcherbina, S. Peregudova, G. Cherkaev, S. N. Chvalun, C. J. Brabec, S. Ponomarenko, *J. Mater. Chem. C* **2016**, *4*, 7061.
[59] Y. N. Luponosov, J. Min, A. N. Solodukhin, O. V. Kozlov, M. A. Obrezkova, S. M. Peregudova, T. Ameri, S. N. Chvalun, M. S. Pshenichnikov, C. J. Brabec, S. A. Ponomarenko, *Org. Electron.* **2016**, *32*, 157.
[60] C. Cui, J. Min, C.-L. Ho, T. Ameri, P. Yang, J. Zhao, C. J. Brabec, W.-Y. Wong, *Chem. Commun.* **2013**, *49*, 4409.
[61] J. Min, Y. N. Luponosov, N. Gasparini, L. Xue, F. V. Drozdov, S. M. Peregudova, P. V. Dmitryakov, K. L. Gerasimov, D. V. Anokhin, Z.-G. Zhang, T. Ameri, S. N. Chvalun, D. A. Ivanov, Y. Li, S. A. Ponomarenko, C. J. Brabec, *J. Mater. Chem. A* **2015**, *3*, 22695.
[62] Y. N. Luponosov, J. Min, A. V. Bakirov, P. V. Dmitryakov, S. N. Chvalun, S. M. Peregudova, T. Ameri, C. J. Brabec, S. A. Ponomarenko, *Dyes Pigm.* **2015**, *122*, 213.
[63] J. Min, Y. N. Luponosov, D. A. Khanin, P. V. Dmitryakov, E. A. Svidchenko, S. M. Peregudova, J. D. Perea, L. Grodd, S. Grigorian, S. N. Chvalun, S. A. Ponomarenko, C. J. Brabec, *unpublished*.
[64] T. S. van der Poll, J. A. Love, T. Q. Nguyen, G. C. Bazan, *Adv. Mater.* **2012**, *24*, 3646.
[65] S. Alem, S. Wakim, J. Lu, G. Robertson, J. Ding, Y. Tao, *ACS Appl. Mater. Interfaces* **2012**, *4*, 2993.
[66] F. J. Lim, A. Krishnamoorthy, G. W. Ho, *ACS Appl. Mater. Interfaces* **2015**, *7*, 12119.
[67] Q. Zhang, B. Kan, F. Liu, G. Long, X. Wan, X. Chen, Y. Zuo, W. Ni, H. Zhang, M. Li, Z. Hu, F. Huang, Y. Cao, Z. Liang, M. Zhang, T. P. Russell, Y. Chen, *Nat. Photonics* **2015**, *9*, 35.
[68] C. J. Schaffer, C. M. Palumbiny, M. A. Niedermeier, C. Jendrzejewski, G. Santoro, S. V. Roth, P. Muller-Buschbaum, *Adv. Mater.* **2013**, *25*, 6760.
[69] M. Jorgensen, K. Norrman, S. A. Gevorgyan, T. Tromholt, B. Andreasen, F. C. Krebs, *Adv. Mater.* **2012**, *24*, 580.
[70] J. Min, Y. N. Luponosov, Z.-G. Zhang, S. A. Ponomarenko, T. Ameri, Y. Li, C. J. Brabec, *Adv. Energy Mater.* **2014**, *4*, 1400816.
[71] W. Ni, X. Wan, M. Li, Y. Wang, Y. Chen, *Chem. Commun.* **2015**, *51*, 4936.
[72] J. Min, Y. N. Luponosov, N. Gasparini, M. Richter, A. V. Bakirov, M. A. Shcherbina, S. N. Chvalun, L. Grodd, S. Grigorian, T. Ameri, S. A. Ponomarenko, C. J. Brabec, *Adv. Energy Mater.* **2015**, *5*, 1500386.

